Solid state opto-impedance of LiNiVO$_4$ and LiMn$_2$O$_4$

**P Kalyani, S Sivasubramanian, S Naveen Prabhu,
K Ragavendran, N Kalaiselvi, N G Ranganathan, S Madhu,
A SundaraRaj, S P Manoharan and R Jagannathan**[1]

Central Electrochemical Research Institute, Karaikudi-630006, Tamil Nadu, India

E-mail: jags57_99@yahoo.com

Abstract
Spinel type LiMn$_2$O$_4$ and inverse spinel LiNiVO$_4$ systems serve as
standard cathode materials or potential cathode systems for application
in high energy density lithium-ion batteries. Upon photo-excitation using
UV radiation of energy ∼5 eV, the LiNiVO$_4$ system shows significant
modification in the solid state impedance pattern while the LiMn$_2$O$_4$
system does not. This study has revealed a significant difference in the
opto-impedance pattern for LiNiVO$_4$ with respect to LiMn$_2$O$_4$,
which may be due to the different electronic processes involved.
An attempt has been made to study this behaviour from the solid-state
viewpoint.

1. Introduction

LiNiVO$_4$ having inverse *spinel* structure (space-group $Fd\bar{3}m$),
which is a new entrant, exhibits the distinct feature of offering
high open circuit cell voltage of ∼4.8 V versus Li and finds
potential application as a cathode system for high-density
lithium batteries [1]. However, several shortcomings such
as low initial discharge capacity, pronounced capacity fading,
sudden drop in cell voltage and the high temperature required
to achieve chemical purity, etc limit the scope of LiNiVO$_4$
systems for battery applications [2]. On the other hand, many
of these shortcomings can be addressed by using a *spinel* type
LiMn$_2$O$_4$ cathode system at the cost of a lower cell voltage of
4.0 V when used in Li-ion batteries [3]. In our opinion many
important electrochemical features in the Li-battery system
cannot be satisfactorily explained by taking into account
the current information available related to Li-intercalation/
de-intercalation processes alone. Furthermore, we believe
that, electronic transitions centring around transition metal
species are also equally important to distinguish between the
performance and electrochemical features of various cathode
materials used in the fabrication of Li batteries. Results of the
present study related to photo-induced impedance (we prefer
to call this '*opto-impedance*') on dry pellets made from both
LiNiVO$_4$ and LiMn$_2$O$_4$, which are used as cathode materials

for Li batteries, will demonstrate this point. It is also significant
to note that the performance of Li batteries is determined
by the choice or chemical composition of the cathode
system.

Recently, it has been found that upon photo-excitation
using UV radiation in the energy range 4–5 eV, the LiNiVO$_4$
system showed a significant modification in the solid-state
impedance pattern, especially in the low frequency region
(∼10 Hz), while the *spinel* LiMn$_2$O$_4$ did not show any such
change [4]. This difference in the opto-impedance pattern
can be considered to be of electronic origin, stemming from
electronic transitions around transition metal ions.

The Nernst equation emphasizes the importance of redox
species in determining the electrochemical cell voltage. In
lithium batteries, free energy considerations based on the
Nernst equation indicate that about 4–5 eV energy is involved
in providing the open circuit cell voltage [5]. Hence, it
is reasonable to assume that the cathode material (in the
form of pellets) when exposed to UV radiation of energy
4–5 eV will simulate conditions comparable to that in a
complete electrochemical system, except for the electrolyte
and electrode–electrolyte interface parts. Furthermore, it
should be noted that photo-excitation using UV radiation could
selectively activate electronic transition(s) in the pellet made
of cathode material(s), which are otherwise not possible in
an electrochemical cell due to the presence of an electrolyte
medium.

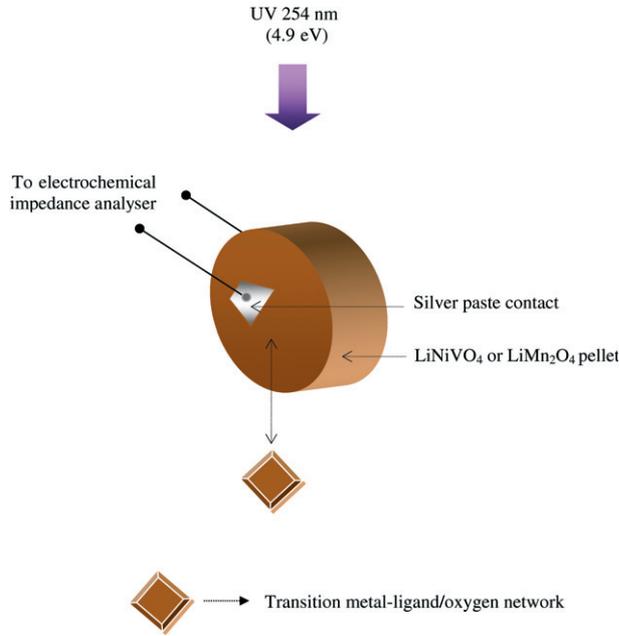[1] Author to whom any correspondence should be addressed.

Figure 1. Schematic illustration of the photo-induced impedance measurement condition on the LiNiVO$_4$/LiMn$_2$O$_4$ pellet.
(This figure is in colour only in the electronic version)

2. Experimental

Experimental procedures pertaining to the synthesis and photo-induced impedance studies on LiNiVO$_4$ and LiMn$_2$O$_4$ samples studied in this investigation were the same as described before [4]. Polycrystalline samples were prepared using the urea-nitrate combustion method. Chemical purity of the synthesized samples was confirmed using the powder XRD method. The XRD patterns and the corresponding least-squares refined crystallographic unitcell parameter values obtained were consistent with standard JCPDS files #18-0736 (LiMn$_2$O$_4$) and #38-1395 (LiNiVO$_4$).

In this study, photo-induced solid-state impedance measurements made on these pellets can be schematized as given in figure 1. Polycrystalline LiMn$_2$O$_4$ and LiNiVO$_4$ samples were made into dry pellets (18 mm in diameter and 2 mm thick) and were used for the impedance measurements. In order to establish electrical (Ohmic) contacts for impedance measurements, a small portion (2 mm diameter) of the pellets was coated with silver paste on either side. The impedance measurements were made using an EG&G instrument (Model #5210 Princeton Applied Research, USA) while UV rays having wavelengths $\lambda = 254$ or 365 nm were used to irradiate the pellet. To ensure the stabilization of photo-generated carriers, before commencing the impedance measurements, an activation time of 2 min after switching on the UV lamp was given. Also, it was found that upon UV exposure there was no appreciable change in the temperature of the pellets.

3. Results and discussion

3.1. Open circuit voltage and lithium intercalation voltage

Dry pellets made of cathode materials were investigated and hence the question of silver contacts affecting the pellet or

reacting with lithium species did not arise. It should be further noted that UV radiation cannot penetrate through the bulk of LiNiVO$_4$/LiMn$_2$O$_4$ pellets. Hence, photo-excitation using UV radiation is expected to cause only surface effects. We interpret only the difference in the solid-state impedance data between UV exposed and unexposed conditions. Hence, conclusions drawn on the basis of differences between the two cases can clearly be attributed to photo-generated electron carriers.

In a lithium cell, the open circuit voltage (OCV) is given by the difference between the chemical potentials of Li in the anode and cathode [5]

$$V(x) = \mu_{\text{Li}}^{\text{anode}} - \frac{\mu_{\text{Li}}^{\text{cathode}}(x)}{zF}, \qquad (1)$$

where F and z, denote, respectively, the Faraday constant and electronic charge transported by the lithium ion to the electrolyte. Hence, when the lithium cell is electrochemically discharged (lithiation), the cell-voltage may decrease primarily due to an increase in the chemical potential of lithium species in the cathode system. Based on topotacticity considerations it can be expected that as electrochemical cycling proceeds, structural changes taking place in the host system will be minimum [6]. This is followed by the Li $\rightarrow$ Li$^+$ transition (and vice versa) for which the electronic charge has to be created for charge compensation. The cell voltage (E) of an electrochemical system can be related to the redox species by the Nernst equation [7]:

$$E = E^0 + \frac{RT}{nF \ln(a_{\text{ox}}/a_{\text{red}})}, \qquad (2)$$

where a_{ox} and a_{red} are essentially the concentration of products of an electronic process related to oxidation/reduction occurring in the transition metal species. Hence, the importance of redox species in determining the cell voltage can be seen. Apart from Li /Li$^+$ species, we can also expect a redox process centring around transition metal ions such as Mn$^{3+/4+}$, Ni$^{2+/4+}$, V$^{3+/5+}$. The important point is that, the former redox process based on lithium species occurs in the vicinity of cathode– and anode–electrolyte interfaces, whereas the latter redox process may occur in the first coordination sphere surrounding the transition metal ion(s).

In our opinion, the LiNiVO$_4$ system involving two transition metal species (Ni and V) may fall under a different category as compared to the spinel LiMn$_2$O$_4$ system. Hence, the former can show increased propensity for oxidation–reduction based charge-transfer transitions. It is natural to ask, whether or not electrons generated through charge compensating or transfer processes can participate in the electrochemical reaction, in particular via metal/ion–ligand in the form of an electronic charge-transfer reaction. But information concerning electronic transitions is not available in the literature. It is pertinent to note that in view of thermodynamic stability considerations, the electrolyte, cathode and anode are designed in such a way that the Fermi levels of the anode and the cathode are much lower than the band-gap of the electrolyte [6]. Thus, in an electrochemical cell system, any free-electron transport through the electrolyte is hardly realized. Also, the importance of stabilization

of higher oxidation state(s) of transition metal ion(s) in determining high-cell voltage has been demonstrated [6]. Hence, time-constant data related to electrokinetic effects of the transition metal redox species may throw some light on the difference between various cathode materials. Furthermore, it has been shown that in a Li-electrochemical cell using a sulfide based cathode, voltages higher than 4 V are not possible [8]. This has been attributed to the location of the 3p electronic level of more covalent S species much above the 2p electron energy level of the O species of an oxide based cathode(s).

3.2. Transition metal ⇔ oxygen/ligand electron-transfer transitions

In Li batteries using different cathode systems, several mechanisms, such as Jahn–Teller (J–T) distortion [9, 10], manganese dissolution in electrolyte [11], loss of crystallinity during cycling [12], formation of two cubic phases of the cathode [13], have been proposed to explain the capacity fading mechanism. Among these, the J–T distortion mechanism in cathode(s) is the most important. This is a consequence of valency change in the transition metal ion(s) constituting the cathode material. In the cubic $LiMn_2O_4$ system upon cell discharging, the tetravalent manganese ion (Mn^{4+}) gets reduced to a trivalent ion (Mn^{3+}) concurrent with the lattice symmetry undergoing a cubic to tetragonal distortion. Now, the pertinent question is, whether the transition metal ion(s) shows any ligand ⇔ metal electron transfer type charge-transfer transitions and if this would influence the electrochemical properties? In any case, such a transition being governed by the inter-ion charge-transfer process, the parity (hence the crystal symmetry) and angular momentum selection rules may not be rigorous. On the other hand, the electronic configuration of the transition metal ion may be more important in determining such charge-transfer transitions. The most important point is, whether the change in valency of the transition metal ion(s), observed through electron transfer following electrochemical cycling, is localized within the first coordination sphere of the transition metal–ligand network or delocalized, suggesting distribution of electrons throughout the bulk of the cathode system. Also, it should be noted whether the electronic charge created consequent to electrochemical cycling (insertion/de-insertion of Li^+ ion) is distributed throughout the unit cell of the cathode system. In any case, the issue concerning the distribution of electronic charge following the insertion of $Li^+ ⇔ Li$ is still not very clear [5]. Hence, we consider, whether any suitable technique focusing on electronic transitions could be employed, and whether it could serve as a means to gain some further insight into the electrochemical properties of the cathode system. Hence, we propose that optical spectroscopic techniques involving electronic transition in the UV–visible region (~ 5 eV) will be more appropriate for this purpose. Owing to the ionic nature of Li^+, any electron transfer reaction between Li^+ ion and ligand(s) constituting the first coordination sphere surrounding the ionic lithium may not be possible. In contrast, in the case of a transition metal–ligand first coordination sphere, an electron transfer may be possible as the bonds are more covalent and spatially extended to facilitate such an electron transfer.
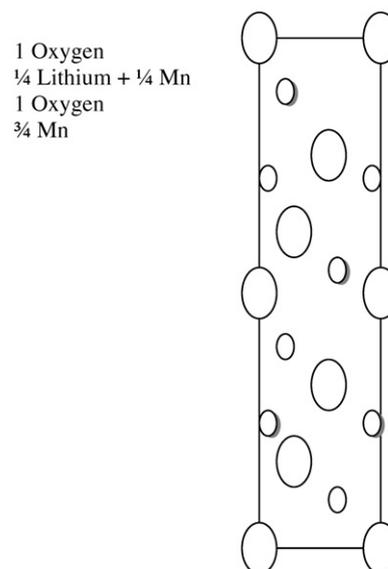

Spinel structure

1 Oxygen
¼ Lithium + ¼ Mn
1 Oxygen
¾ Mn

Figure 2. Normal spinel: $Li[Mn_2]O_4$ (space-group: $Fd\bar{3}m$): tetrahedral site: Li^+, octahedral site: $Mn^{3+/4+}$. Inverse spinel: $V[LiNi]O_4$ (space-group: $Fd\bar{3}m$): tetrahedral site: V^{5+}, octahedral site: Li^+ and Ni^{2+}.

Structurally, $LiMn_2O_4$ and $LiNiVO_4$ adopt spinel and inverse spinel structures, respectively, and are quite similar in their lattice symmetries ($Fd\bar{3}m$). The difference arises only in site(s) occupancy of the transition metal (Mn^{2+}/Ni^{2+}) and Li ions being interchanged between octahedral O_h and tetrahedral T_d sites as indicated in figure 2.

3.3. Photo-induced impedance of $LiNiVO_4$ vis-à-vis *the* $LiMn_2O_4$ *system*

The importance of electronic transfer (rather electronic transition(s) to be more specific) in determining electrochemical properties of the lithium battery system has been well recognized recently [14]. Electronic band-structure considerations based on molecular orbital calculations on a cathode system indicate an energy gap of about 3–5 eV between HOMO and LUMO orbitals constituted by the d- and p-orbitals of transition metal ion(s) and anions (usually O^{2-}), respectively. The opto-impedance spectra (Bode and Nyquist plots) of $LiMn_2O_4$ and $LiNiVO_4$ samples both under UV and without exposure are given in figures 3–6 and the results obtained from this are consolidated in table 1. The impedance spectra can be split into two parts comprising an impedance component under no UV condition (Z_1) and the new component generated upon UV exposure (Z_2). In the case of the Nyquist plot, UV exposure caused significant difference in the Z_1 impedance values and the differences between dark and UV exposed conditions are given as ΔZ in table 1.

Figures 3 and 4 depict Bode impedance plots of $LiMn_2O_4$ and $LiNiVO_4$ cathode systems, respectively, measured both with and without UV exposure. Upon excitation using UV radiation, the impedance spectrum of the $LiMn_2O_4$ system maintains a nearly similar pattern as that of the unexposed sample. This means that under photo-excitation, the Bode plot corresponding to the *spinel* $LiMn_2O_4$ system shows
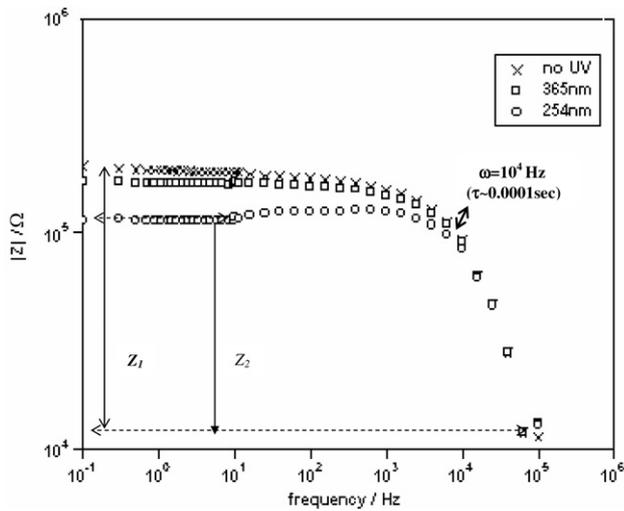
Figure 3. Bode impedance plots of LiMn$_2$O$_4$ pellet with and without UV exposure. Total impedance Z_1 (under no UV) and Z_2 (with UV irradiation) are indicated.
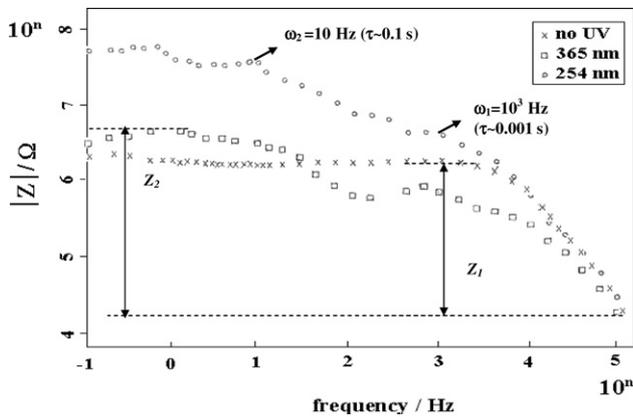

Figure 4. Bode impedance plots for the LiNiVO$_4$ pellet with and without UV irradiation. Total impedance Z_1 (under no UV) and Z_2 (under UV irradiation) and also time constants (τ) are indicated.

no visible change in the impedance spectrum with respect to the unexposed sample, except for a slight decrease in the impedance value near the low frequency region around 10 Hz (figure 3, table 1), while for the LiNiVO$_4$ system, upon UV exposure, the impedance spectrum becomes more complex with respect to the unexposed sample, suggesting the generation of multiple photo-generated species. With no UV exposure, the Bode plot of the LiNiVO$_4$ system looks nearly the same as that of LiMn$_2$O$_4$. Upon UV exposure (particularly 254 nm UV irradiation) the LiNiVO$_4$ system shows a more complex pattern comprising at least two steps in the low frequency regions centred around 10 Hz and 1 kHz. Thus, the impedance spectrum corresponding to LiNiVO$_4$ presented in figure 4 can be divided into several parts and labelled as Z_1, Z_2 for different frequency regions, whereas for the LiMn$_2$O$_4$ there is only one component, Z_1.

Now, turning to the Nyquist plots (figures 5 and 6), the *spinel* LiMn$_2$O$_4$ system under no UV exposure shows an asymmetric semicircle showing an impedance value of $Z_1 = 195$ kΩ. Upon UV irradiation, the semicircular pattern gets more symmetric with the central frequency shifting

towards lower impedance values decreased by 40%, with an impedance value of $Z_2 = 120$ kΩ. The skewed semicircular impedance pattern observed for the unexposed LiMn$_2$O$_4$ sample suggests the possibility of another pattern/component being superimposed on the semicircle. In the case of the LiNiVO$_4$ system, with no UV exposure, we obtain a somewhat semicircular impedance pattern with an impedance value of about $Z_1 = 2$ MΩ, while upon UV exposure two semicircles appear exhibiting larger impedance values (table 1). Under the Nyquist *plot*, a simple semicircular impedance pattern can be rationalized in terms of silver contacts constituting a capacitor with the dielectric LiMn$_2$O$_4$ across it leading to a resistor and a capacitor in parallel. Also, the decrease in impedance observed upon short UV can be attributed to an increase in photo-generated carriers (electrons). On the other hand, in the case of LiNiVO$_4$ the impedance pattern becomes more complex (figure 6). This may be roughly described by two semicircles with the first one essentially being the same as that under dark conditions and can be attributed to silver contacts. The emergence of a second semicircular pattern, in particular, may suggest a new phase element in the form of a resistor–capacitor in parallel. Also, there is a significant increase in the imaginary part of the impedance value in contrast to the *spinel* system, which may be explained as being due to enhancement in capacitative impedance.

Also, it should be noted that a semicircular Nyquist plot in the low frequency region may characterize a charge-transfer process [15]. From the conventional electrochemical impedance studies, it is known [14] that Li$^+$ insertion and de-insertion and the associated interfacial charge-transfer processes taking place in a lithium battery system exhibit a very low impedance value of about 100 Ω, whilst the present opto-impedance studies made on LiNiVO$_4$/LiMn$_2$O$_4$ dry pellets show a very large impedance value of several kiloohms to megaohms. Such a large difference in the impedance values may be explained in terms of a large difference in sample dimensions, configuration and more importantly the configuration of the impedance set-up used, such as impedance measurement made on dry solid pellets without electrolyte medium, etc.

The Bode plot corresponding to the LiNiVO$_4$ system clearly points to the involvement of low frequency components (10 Hz–1 kHz region) having a profound dependence on photo-excitation conditions. In the case of LiMn$_2$O$_4$, the decrease in impedance value observed may be attributed to photo-generated electronic charge carriers. Notwithstanding this general trend, an increase in impedance observed for the case of LiNiVO$_4$ at low frequencies ($\sim$10 Hz) is intriguing, which may be due to the generation of a new kind of impedance component.

Results of the present opto-impedance study can be represented with the help of equivalent circuit diagrams as given in figures 5 and 6. For the spinel LiMn$_2$O$_4$, the picture is simple i.e. capacitance (C_1), due to silver contacts or the dielectric medium of the pellet in series with a linear resistance (R_1), puts up a total impedance $1/Z_1 = jC_1\omega + 1/R_1$. Upon UV exposure, there is a linear decrease, probably lowering the linear resistance part ($R_1 - x$), with x corresponding to the decrease in Ohmic resistance, which would appear as impedance $1/Z_2 = jC_1\omega + 1/R_1 - x$.
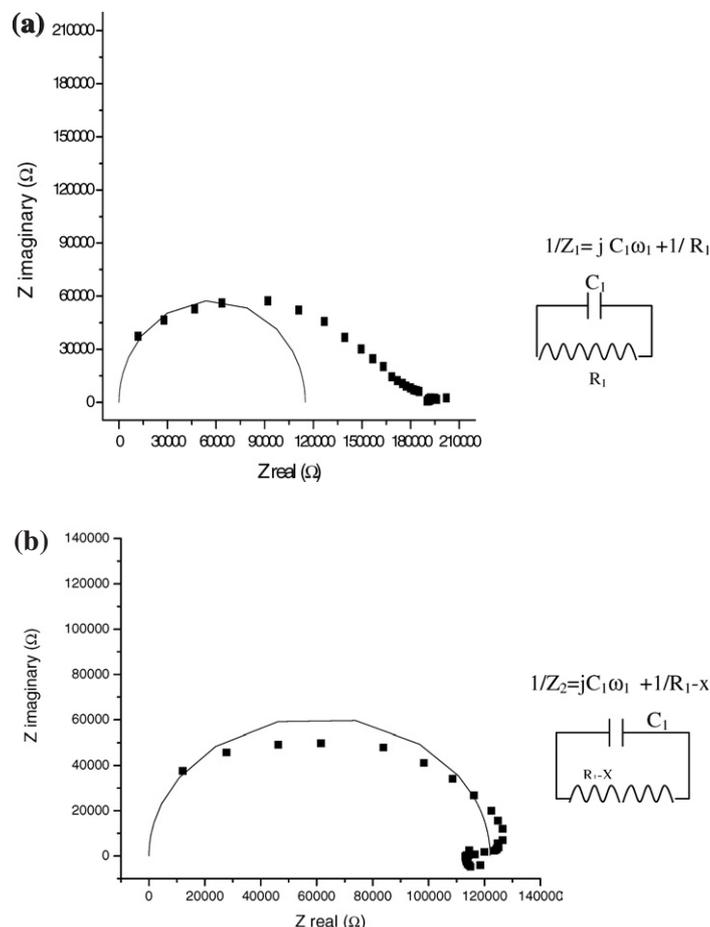
Figure 5. Nyquist impedance plot of LiMn$_2$O$_4$ under (*a*) dark conditions and (*b*) with UV (254 nm) exposure (······: experimental; ——: fitted).

In the case of the LiNiVO$_4$ system, the impedance pattern becomes more complex. Under normal conditions with no UV exposure, a simple capacitance plus a resistor in parallel due to the bulk material and silver contacts make the impedance $1/Z_1 = jC_1\omega + 1/R_1$ when a high frequency is realized. Upon UV exposure, the equivalent circuit of LiNiVO$_4$ can be attributed to a capacitance plus resistor network in parallel with a new capacitor element C_2 generated along with resistive impedance (R_2) showing higher impedance. This means that in addition to the capacitance at higher frequency ($\omega_1 = 10$ kHz) due to silver contacts, another capacitance as well as resistor components in parallel, at lower frequency ($\omega_2 = 10$ Hz), would be possible.

In order to check the validity of the equivalent circuits proposed, these data were fitted using theoretical values as given in table 1. As can be seen from figures 5 and 6, there is a close agreement between experimental (dotted line) and theoretical curves (solid lines) for the case of LiMn$_2$O$_4$ and also for LiNiVO$_4$ under dark conditions. However, we could not achieve a successful fitting for the case of LiNiVO$_4$ under UV exposure. This is because of the emergence of an additional complex pattern. Further studies are necessary to gain more insight into this, and are under way. Moreover, time constant data deduced from different frequency regions may lead to some interesting clues about the nature of the transitions involved.

In the case of the LiNiVO$_4$ system, the occurrence of charge-transfer transition(s) having slow kinetics $(10 \text{ Hz} = 10 \text{ s}^{-1} = 0.1 \text{ s})$ seems to be possible, while the LiMn$_2$O$_4$ system does not show such transition(s). In order to explain this, we should consider different possibilities. We reject outright the possibility that these transitions can have an ionic origin related to Li$^+$/Li insertion/de-insertion charge-transfer transition, because such transitions are known to occur only in the region of the electrode–electrolyte interface. On the other hand, these transitions can have an electronic origin, which show up when energized suitably, in particular optically. Energy considerations for these transitions suggest that these can be attributed to well-localized transition metal ion(s)–ligand electron-transfer transitions [16]. These transitions may be located within the first coordination sphere constituted by the O^{2-} ions around the transition metal ion(s).

In the Nyquist plot, upon UV exposure, the evolution of a complex pattern almost corresponding to two semicircles with different time constants (0.1 and 0.001 s) is a clear indication of some photoelectron processes. If we consider these electronic transitions, some insights into hitherto unexplained electrochemical properties of these cathode materials may be possible. Hence, it seems reasonable to propose that the metal–ligand electron-transfer transition in the first coordination sphere around the transition metal species is as important as the Li-ionic part in determining the cell voltage and other allied electrochemical properties.
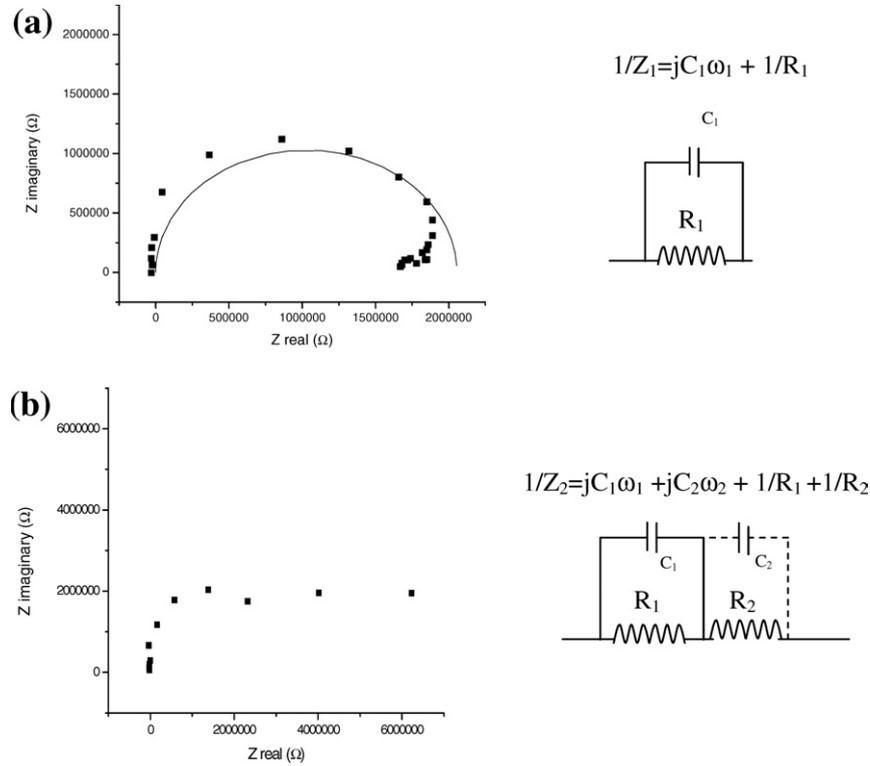
Figure 6. Nyquist impedance plot of LiNiVO$_4$ under (*a*) dark condition and (*b*) with UV (254 nm) exposure (·····: experimental; ——: fitted).

Table 1. Photo-induced impedance data of LiNiVO$_4$ and LiMn$_2$O$_4$ systems.

Cathode system	UV exposure condition (λ_{UV})	Photo-induced impedance (experimental)				Photo-induced impedance (ΔZ) using Nyquist	Fitted impedance (theoretical)	
		Bode		Nyquist				
		Z_1	Z_2	Z_1	Z_2		R	C
LiMn$_2$O$_4$	No UV	180 kΩ	—	180 kΩ	—	—	115 kΩ	4.09×10^{-4} μF
								4.62×10^{-4} μF
	254 nm	100 kΩ	—	130 kΩ	—	50 kΩ (−)	122 kΩ	—
	365 nm	130 kΩ	—	170 kΩ	—	10 kΩ (−)	—	—
LiNiVO$_4$	No UV	1.98 MΩ	—	1.95 MΩ	—	—	2.05 MΩ	3.6×10^{-4} μF
	254 nm	4.98 MΩ		3.52 MΩ	3.21 MΩ	1.57 MΩ (+)	—	—
		20.0 MΩ[a]						
	365 nm	0.78 MΩ		0.93 MΩ	2.12 MΩ	1.02 MΩ (−)	—	—
		3.2 MΩ						

[a] Some additional process also seems to be occurring.

(−) indicates decrease in impedance; (+) indicates increase in impedance.

4. Conclusions

The solid-state impedance spectra obtained under UV excitation of LiNiVO$_4$ and LiMn$_2$O$_4$ cathode pellets have revealed some definite photo-dependent process. In the LiNiVO$_4$ system, the UV induced semicircular impedance pattern (under the Nyquist plot) with a large impedance value ($Z_2 \sim$ 4–20 MΩ), having slow kinetics (0.1 s), may correspond to a capacitative impedance arising from a charge-gradient generated from photo-electronic species. This may serve as a key to understanding hitherto unexplained properties, such as high open circuit cell voltage in lithium batteries when employing the LiNiVO$_4$ cathode system. Although the UV excitation can only induce electronic transitions limited to a few atomic layers, for all practical purposes this can be considered to represent the behaviour of the bulk cathode system because cathode materials are coated as thin films in practical applications.

Acknowledgments

References

[1] Fey G T K, Li W and Dahn J R 1994 *J. Electrochem. Soc.* **14** 2279

[2] Lu C H and Liou S J 2000 *Mater. Sci. Eng.* B **75** 38

[3] Ohzuku T 1994 *Lithium Batteries* ed G Pistoia (New York: Elsevier) chapter 6

[4] Kalyani P, Jagannathan R, Gopukumar S and Lu C H 2002 *J. Power Sources* **109** 301

[5] Ceder G, Aydinol M K and Kohan A F 1997 *Comput. Mater. Sci.* **8** 161

[6] Manthiram A and Kim J 1998 *Chem. Mater.* **10** 2895

[7] Rubinstein I (ed) 1995 *Physical Electrochemistry: Principles, methods & Applications* (New York: Marcel Dekker) chapter 1

[8] Goodenough M, Manthiram A, James A C W P and Strobel P 1989 *Mater. Res. Soc. Symp. Proc.* **135** 391

[9] Ozhuku T, Kitagawa M and Hirai T 1990 *J. Electrochem. Soc.* **137** 769

[10] Sun Y K and Jeon Y S 1999 *J. Mater. Chem.* **9** 3147

[11] Inoue T and Sano M 1998 *J. Electrochem. Soc.* **145** 3704

[12] Kannan A M and Manthiram A 2002 *Electrochem. Solid State Lett.* **5** A167

[13] Xia Y and Yoshio M 1996 *J. Electrochem. Soc.* **143** 825

[14] Oliver-Fourcade J, Jumas J-C and Connerade J-P 1999 *J. Solid State Chem*. **147** 85

[15] Levi M D, Gamolsky K, Aurbach D, Heider U and Oesten R 2000 *Electrochim. Acta* **45** 1781

[16] McClure D S 1959 *Solid State Physics* ed F Seitz and D Turnbull (New York: Academic) vol 9, chapter 5